November 1996

Optical Materials 6 (1996) 331–338

Concentration effects on the IR-luminescent channels for Er- and Ho-doped $LiYF_4$ crystals

Marly B. Camargo *, Laércio Gomes, Izilda M. Ranieri

Instituto de Pesquisas Energéticas e Nucleares, Caixa Postal 11049, Pinheiros, 05422-970 São Paulo, Brasil

Received 12 February 1996; accepted 17 July 1996

Abstract

In this paper we report the ideal concentrations for the main infrared laser channels of the Er^{3+}- and Ho^{3+}-doped $LiYF_4$ (YLF) crystals, under Xe lamp pumping. The number of photons per luminescent element are also checked for laser lines. It was determined that 10–30% of Erbium is the ideal concentration for laser action at 2.74 μm, as well as the 1.2% Er-doped YLF crystal is the best one for lasing at 0.88, 1.23, and 1.72 μm under flashlamp pumping. The present method is a good approach in order to indicate the ideal concentration for an optimized four-level laser system. For the transitions at 1.63 μm (Er:YLF) and at 2.07 μm (Ho:YLF) it was observed that the luminescence intensities are maximized in the concentration range (25–35)% for Er laser and in the range (10–15)% for Ho ions in the YLF crystals. Nonetheless, these concentration values are much higher than the ones used in a practical three-level laser system.

1. Introduction

The lasers based on the rare-earth (RE^{3+}) ion transitions in crystals are very useful for a large number of applications in industry, [1–4] science, [5,6] medicine, [7–10] communications, civil and air defense [11,12]. Among these lasers, the ones based on Er^{3+} and Ho^{3+} are important because of their laser transitions, which run from 0.80 to 3.00 μm. The overlapping of the water absorption spectrum with these laser emissions at 2.94 μm (Er:YLF) and 2.07 μm (Ho:YLF), makes them very convenient as medical tools for cutting, dentistry, and other medical procedures where the lasers interact directly with the biological tissues, whose composition is mainly water.

In a previous work, we studied the temperature dependence of the Er and Ho ions luminescence in $LiYF_4$ crystals [13,14] for low and high dopant concentration. Pumping the $^4G_{11/2}$ manifold of low Er-concentration crystals at 77 K, the most intense luminescences are: $^4S_{3/2} \rightarrow {}^4I_{15/2}$ at 548 nm and $^4S_{3/2} \rightarrow {}^4I_{13/2}$ at 847 nm. On the other hand, at a higher concentration (38.5%), these transitions are quenched by both temperature (room temperature) and concentration and therefore, the other mid-infrared luminescent channels, beyond 850 nm, are the main contributors to the total luminescence of this laser material. For the Ho:YLF crystals, the high concentration effect introduces the quenching of the visible transitions favoring the transitions at 1.3 μm ($^5I_6 \rightarrow {}^5I_8$) and at 2.1 μm ($^5I_7 \rightarrow {}^5I_8$).

* Corresponding author.

PII SS925-3467(96)00083-1

Although that previous work demonstrated laser temperature and a drastic change in the dopant concentration affects the luminescence of these laser materials, the effects of the activator concentration variation on the luminescence of the main laser transitions of Er^{3+} and Ho^{3+} ions in $LiYF_4$ crystals were not investigated.

Pumping the Er and the Ho:$LiYF_4$ crystals with the white light from a Xe lamp, one determines the crystal behavior under a flashlamp pumped laser resonator, where almost all the transitions of the activator are excited (see Fig. 1 for the Er:$LiYF_4$). In the present work, the active ion (Er, Ho) concentration in the YLF crystals was varied, keeping the same pumping conditions in order to verify the best concentrations for each laser transition.

In order to make it clear that the determination done in this work is valid we included another figure (Fig. 2), showing the spectrum of our Xe cw lamp (Cermax Xe, model LX300UV, 300 W) with an IR filter (Schott glass KG-3) and also that one referring to a common ILC Xe flashlamp [15] with a current density of 3100 A/cm^2 and gas pressure of 450 Torr [16], used to pump orbitan lasers. The KG-3 filter cuts all wavelengths below 300 nm and shows 1000 nm. This filter one-use together with the Xe lamp, to simulate a flashlamp pumped water cooled laser resonator because the thin film of water which works as a filter for the UV and IR (> 1000 nm) wavelengths. It is important to notice that the flashlamp with the thin film of water presents almost the same spectrum than the one exhibited by the pumping system used in the present work.

2. Experiment

A conventional hydrofluorination procedure utilizing ultra pure rare earth oxides was used to synthesize the starting materials for the crystal growth. The

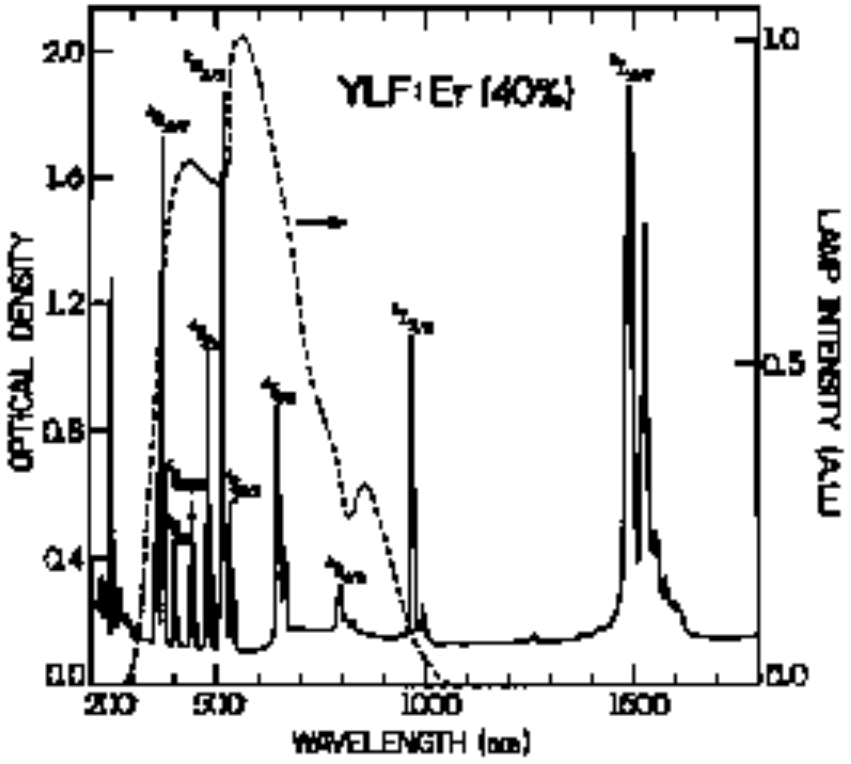

Fig. 1. OM-[illegible]:YLF absorption spectrum at 300 K, referring to the left scale and the Xe lamp plus an KG-3 glass filter (cut-off at 1000 nm) emission which was used to pump the YLF crystals, referring to the right scale. 40.0% was the measured value for the Er-concentration in YLF crystal.

Er or Ho:YLF synthesized material was grown by conventional Czochralski's method under argon atmosphere. Both Ho and Er:YLF batches underwent a thermal treatment prior to sample preparation, to eliminate the steps originated during the growth process. Er doped YLF could be grown in control concentrations from 1 to 100%. On the other hand, during the Ho:YLF crystals growth, the holmium fluoride (HoF_3) could be added to the YLF melt forming a solid solution up to 10% at/at. For higher Ho concentrations, however, there is a solute precipitation due to the YF_3–HoF_3 phase-diagram incongruous; in spite of that the $HoLiF_4$ could be obtained.

After the crystal growth, we selected the regions of the boules free of scattering to extract the samples. The samples used in this study were single crystals of Ho:YLF and Er:YLF with variable RE^{3+}-ion concentration (1.00, 1.42, 2.77, 4.95, 38.5, and 100% for Er-crystals and 1.71, 3.00, 7.00 and 100% for Ho crystals). 2.7 mm thick Er:YLF and 2.0 mm thick Ho:YLF crystals were cut and polished with parallel surfaces for that purpose.

The experimental setup is the same as described

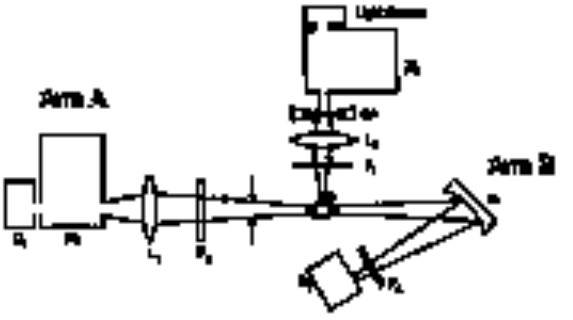

Fig. 3. Experimental setup. D_1 and D_2 are detectors (PMT and/or InSb), M_1 and M_2 are monochromators, Ch is a chopper, S is the sample, L_1 and L_2 are lenses, F_1 is a KG-3 glass filter with a cut-off at 2800 nm, F_2 is KG 780 or a thin Si wafer filter, F_3 is a 2 mm width Ge wafer filter, and F_4 is a Germanium filter (KG—18 cm focal curve radius = 15 cm).

al measures [13] (see Fig. 3). The excitation was provided by the instrument continuous Cermax Xe arcmax model LX300UV plus the KG-3 glass filter, described earlier in the text. In order to minimize the stray-light contribution to the measured signal, the measurements were taken at 90° from the excitation light-beam. To perform quantitative luminescence

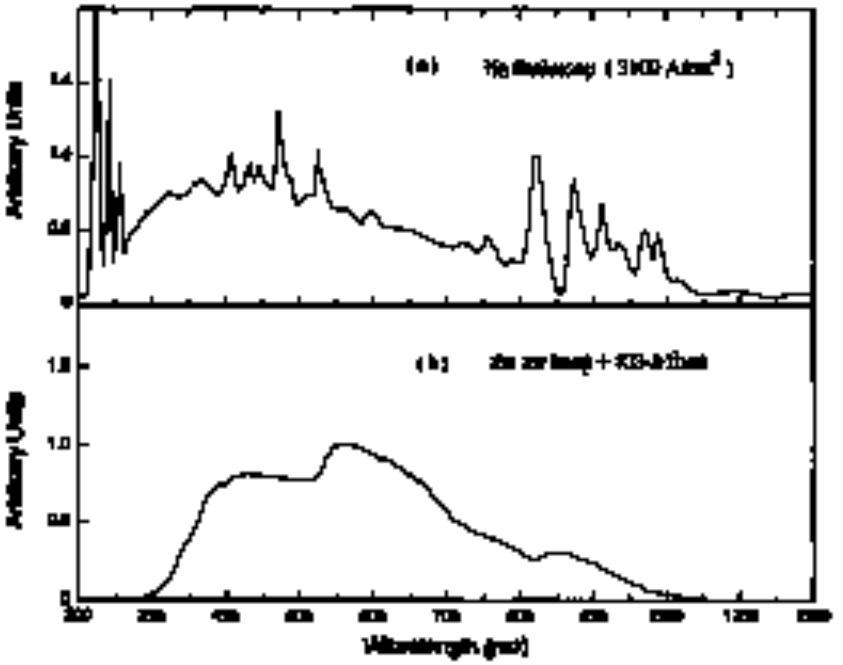

Fig. 4. Excitation spectra of: (a) a detection E.C. Xe flashlamp (4.58 J/cm² and 3900 A/cm²) used to pump 2.0% and 3.0% and (b) a Cermax continuous Xe (300 W) lamp used to pump the Er:YLF crystals in this work.

measurements the excitation and collecting angles in the sample under investigation were kept the same. All the fluorescences, for $\lambda \leq 2.6$ μm, were measured in arm A by using a system composed by a filter F_1 (RG780 or Si filter), a Kratos analyzer monochromator (0.25 m) with slits of 1 mm and a detector D_1 (S-20 extended, S-1 PMT's from EMI or InSb from Judson). These slits were chosen to match the integration interval to the multiplet width under investigation. The only luminescent signal collected in arm B was 2.34 μm because this luminescence was too weak to be observed in arm A. In this case, a collecting mirror was used to focus the light into a detector and a Ge filter was used in front of the detector D_2 (InSb, Judson 510 series), which was cooled at 77 K. The responsivity of all the detectors (in V/W) was obtained using an electrically calibrated pyroelectric radiometer model RK-5900 from Laser Precision, as a reference.

The transmission band-pass of the analyzer monochromator was taken for each luminescent channel in order to correct the values of the luminescence signals. It was a Gaussian shape with a half-width of 12 nm.

The luminescence power, corrected and normalized for each luminescent channel, in Watts, was obtained using the expression:

$$\delta = \frac{S_{\lambda 90}}{ST}, \tag{1}$$

Table 1
Filters used in the experimental setup and the sub-bands the measurement was taken.

Emission range (nm)	Filters use	Filter transmission T (%)	Arm
800–950	BG 780	85	A
1000–2600	Si	50	A
Filter On Er emission at 2740 nm	Ge	45	B

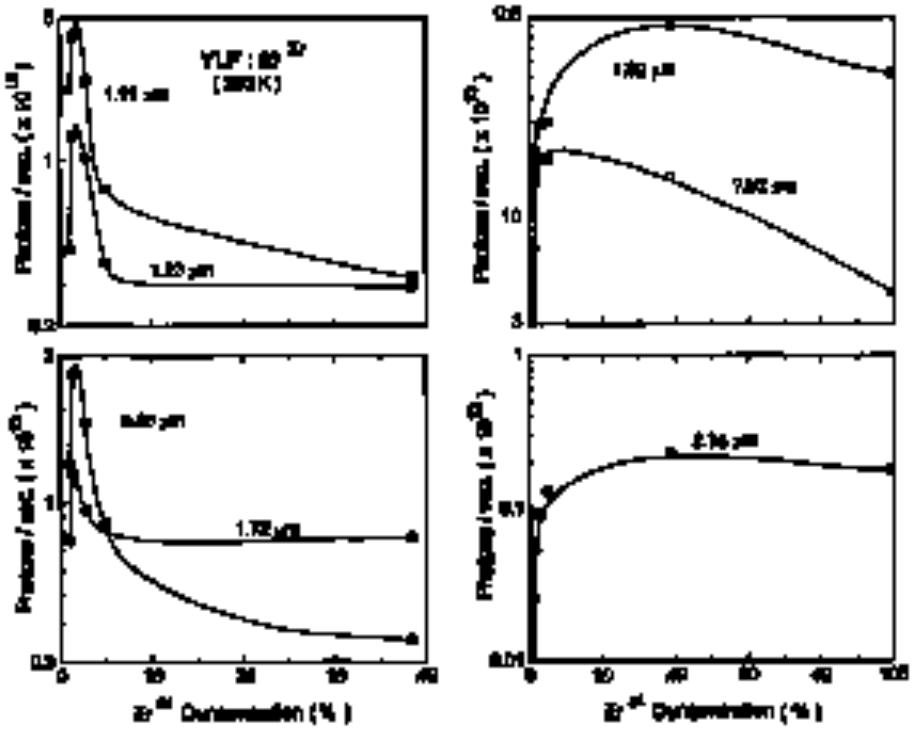

Fig. 4. Number of photons emitted by the Er^{3+} 4f emissions, measured as a function of Er-concentration, the Or ErLiYF$_4$ crystal before a Xe lamp excitation at 300 K. The curves correspond to the following Er^{3+} emissions: 0.82 μm ($^4S_{3/2} \rightarrow {}^4I_{9/2}$); 1.35 μm ($^4S_{3/2} \rightarrow {}^4I_{11/2}$); 1.55 μm ($^4I_{13/2} \rightarrow {}^4I_{15/2}$); 1.11 μm ($^4F_{9/2} \rightarrow {}^4I_{11/2}$); 1.70 μm ($^4S_{3/2} \rightarrow {}^4I_{9/2}$); 1.62 μm ($^4I_{11/2} \rightarrow {}^4I_{13/2}$); and 2.34 μm ($^4I_{11/2} \rightarrow {}^4I_{15/2}$).

where S_i is the measured integrated luminescence signal (in V), g is a correcting factor (defined in Eq. (2)) which takes into account the transmission bandpass of the analyzer monochromator $M_{i,i}$ and g is the ratio between the total solid angle 4π and the one used in area A (in B). R is the detector responsivity (in V/W) and T is the optical transmission of the optical filters used in the experiment. In this method for the integrated luminescence signal measurement correction (δ), the main source of errors are the factors p and g. As a consequence, a typical error of 6% must be considered.

The filters used in the experimental setup as well as the collecting area, where the data were taken, are indicated in Table 1. The KG-3 glass filter, with a cut-off at 1.0 μm, was placed in the excitation light beam path in order to simulate the excitation spectrum of a Xe flashlamp typically used to pump a laser rod inside a laser resonator. The Xe lamp spectrum with the KG-3 glass filter can be seen in Figs. 1 and 2.

The factor g is defined as the ratio between the corrected luminescence signal and the measured one:

$$g = \frac{\sum_i S_i A(\lambda_i)}{\sum_i S_i T_i A(\lambda_i)}, \tag{2}$$

where S_i is the luminescence signal at the wavelength λ_i, T_i is the transmission of the monochromator at the ith-λ value, and $A(\lambda_i)$ is a constant 2 nm wavelength interval at λ_i.

According to Beer's law for a single-ion-absorption, the absorbed power for the ith-channel is proportional to:

$$P_i = P_{in}[1 - \exp(\bar{\alpha}_i d)], \tag{3}$$

where $\bar{\alpha}_i$ is the average absorption coefficient ($\alpha_i = \sigma_i N$, where σ_i is the absorption cross-section and N is the dopant concentration) and d is the crystal thickness.

The total absorbed power is given by:

$$P_t = \sum_i P_i. \tag{4}$$

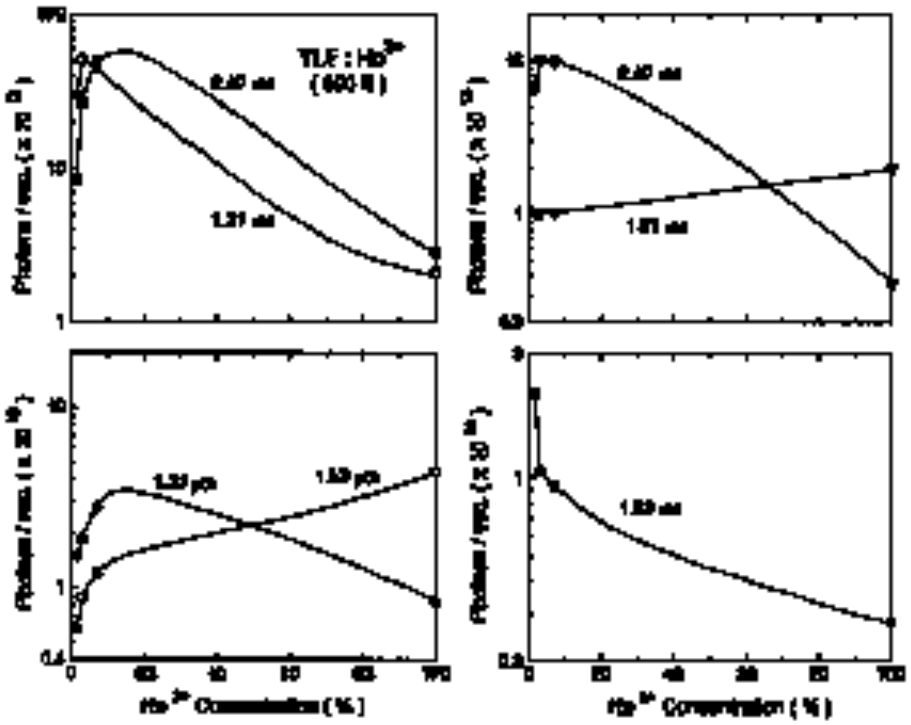

Fig. 2. Number of photons emitted by the Ho^{3+} IR luminescence channels as a function of Ho-concentration, for the Ho:YLF crystals under a Xe lamp excitation at 300 K. The Ho^{3+} transitions corresponding to these curves are: 1.80 μm ($^5F_5 \rightarrow {}^5I_8$); 1.21 μm ($^5I_6 \rightarrow {}^5I_8$); 1.33 μm ($^5S_2 \rightarrow {}^5I_7$); 1.51 μm ($^5F_5 \rightarrow {}^5I_7$); 1.89 μm ($^5I_6 \rightarrow {}^5I_7$); 2.05 μm ($^5I_7 \rightarrow {}^5I_8$); and 0.40 μm ($^5F_1 \rightarrow {}^5I_8$).

where Σ_r is the summation over all the excited transitions for $\lambda \leq 1000$ nm.

3. Results

Using the Eq. (2) in Eq. (1) one obtains the equivalent power for each luminescent channel of Er^{3+} and Ho^{3+} ions. Dividing the power of one channel by its average photon energy, one gets the number of emitted photons per second corresponding to that luminescent channel. The same procedure was adopted for all the luminescent channels studied in this work. Figs. 4 and 5 show the number of photons/s per luminescent channel, for several Er- and Ho-concentrations in YLF crystals. All the measurements were performed at room temperature since laser working at low temperatures are more complicated to be operated, and as one always expects to use a laser which works easily at room temperature.

4. Discussion and conclusions

4.1. Er^{3+}:YLF crystals

4.1.1. Luminescent transitions from the $^4S_{3/2}$ and $^4F_{9/2}$ laser levels

Fig. 4 shows that for low Er-concentration, i.e. from 1 to 2%, the Er^{3+} four-level laser transitions most favored at room temperature are 0.85, 1.11, 1.23, and 1.72 μm. For these transitions the number of photons/s as a function of the Er-concentration peaks at 1.2%, showing that the cross-relaxation processes are very efficient for concentrations above 1.7%, causing the decrease of the population from the $^4S_{3/2}$ and $^4F_{9/2}$ levels. When the Ion concentration increases from a very low value up to 2%, the absorbed power and the emission intensities of the $^4S_{3/2}$ and $^4F_{9/2}$ levels increase. As a consequence, the number of photons emitted by those levels also increase. On the other hand, concentrations above 2% favor the cross-relaxation processes, which depopulate those levels, thus producing the maximum luminescence peak for about 1.7% of Er in $LiYF_4$ crystals and a drastic decrease above this concentration.

Some authors [17–20] studied only the $^4S_{3/2}$ lifetime as function of the Er concentration for the $LiY_{1-x}Er_xF_4$ (where $x = 0.01–1.00$) crystals. Tkachuk et al. [17] indicated that an optimum Er concentration range, for the laser transitions at 0.85 and 1.23 μm, is 2 to 5% of Er:LiYF$_4$ crystals, due to the ion–ion cross-relaxation processes which quench the $^4S_{3/2}$ luminescence. Ramos [18] pointed out that (6%)Er is the most appropriate concentration for a particular Q-switched Er:YLF pulsed laser at 1.73 μm. Pollack et al. [19] used a (5%)Er:YLF crystal to obtain laser active at 0.85, 1.23, and 1.73 μm by upconversion processes. Klatte et al. [20] observed that the laser transition at 1.73 μm is not efficient by a concentration of (2%)Er. On the other hand, concentrations ≥ (4%)Er quench the $^4S_{3/2}$ fluorescence and for a (16%)Er crystal, that laser level is completely quenched. The results presented by Klatte et al. [20] are the closest to the present work (see Fig. 4) for the transitions from the $^4S_{3/2}$ laser level. We observed a similar behavior for the emission at 1.11 μm ($^4F_{9/2} \rightarrow {}^4I_{11/2}$), peaking at (1.7%)Er, which was not studied before, at least to our knowledge.

4.1.2. Luminescent transitions from the $^4I_{11/2}$ and $^4I_{13/2}$ laser levels

Fig. 4 also shows that the emission at 1.62 μm is favored in the 25–35% Er-concentration range, and for the laser emission at 2.74 μm, an Er-doped YLF with 30–40% should be the more convenient candidate.

Studying the Er:YLF emission at 1.62 μm, we observed that the number of photons per second emitted by that channel increased nine times for the (30.5%)Er:YLF system in comparison to the 1% Er-doped one, while the total absorbed power (for white light excitation) increased only by a factor of two. It states that when one increases the Er concentration, the cross-relaxation transfers the population from the $^4S_{3/2}$ and $^4F_{9/2}$ levels to the $^4I_{11/2}$ and $^4I_{13/2}$ ones, enhancing the number of photons emitted by the latter levels by a factor of ~4.5.

It was also observed that for the $^4I_{13/2} \rightarrow {}^4I_{15/2}$ transition at 1.62 μm and, $^4I_{11/2} \rightarrow {}^4I_{15/2}$, at 2.74 μm, the curves corresponding to the number of photons (see Fig. 4) emitted per second as a function of the dopant-concentration show a pronounced initial increase, followed by a saturation for the concen-

tration range from 20 to 40%, and then, slightly decreasing for higher Er concentrations.

According to Auzel et al. [21] the $^4I_{11/2}$ and $^4I_{13/2}$ laser level lifetimes are almost constant for concentrations up to (20%)Er, decreasing rapidly for concentrations higher than (25%)Er, because of the upconversion processes to higher energy levels, causing losses during the 3 μm laser action in Er:YLF. Sardeshida et al. [22] studied the concentration effects in the laser transition at 3 μm for Er:YAG on the concentration range from 0.1 to 100%. Their conclusions are very similar to the ones from Auzel; however, the authors attributed the luminescence quenching observed to power impurities whose concentrations increase with the increase of Er concentration, for ≥ 20%(Er).

We observed a luminescence saturation behavior for concentrations ≥ 10%(Er), for the transitions at 3.74 μm and at 1.62 μm (see Fig. 4), which is expected if $\alpha_{ij}d \gg 1$ in Eq. (3), i.e., this condition is satisfied for this concentration level. The decrease in the number of phonons/s for concentrations above 40% shows that there are power quenching processes occurring. In a previous publication [13,14] we attributed this quenching process to the energy transfer from the levels $^4I_{11/2}$ and $^4I_{13/2}$ of Er^{3+} ions and from the $^5I_4$ and $^5I_7$ of Ho^{3+} ions to the molecular impurities $Mg^{++}(OH^-)$ and CHO^- present in the crystal lattice.

Other effects such as self-quenching or upconversion, besides the energy transfer to sink impurities, must be considered in order to estimate the effective gain of the Er or Ho:YLF laser, mainly in high concentrations. Particularly, taking into account all the considerations above, we can indicate that for the Er laser transition in 3.74 μm, the ideal concentration range is $10\% \leq x \leq 20\%$ (where x is the Er concentration).

4.2. Ho^{3+}:YLF crystals

From Fig. 3 one verifies that the most intense luminescence of Ho^{3+} ions are: 1.21 μm ($^5I_6 \rightarrow {}^5I_8$), 2.00 μm ($^5I_7 \rightarrow {}^5I_8$), 2.40 μm ($^5F_5 \rightarrow {}^5I_8$). While the transitions at 1.00 and at 1.51 μm increase with the Ho concentration, the other luminescences decrease.

The 2.00 μm luminescence ($^5I_7 \rightarrow {}^5I_8$) of the Ho^{3+}:YLF crystals is maximized for concentrations in the range from 10 to 15%. Since that transition represents a three-level laser, such a high concentration would not help to improve the laser action because of the upconversion processes, which adds a lot of population to the higher Ho levels, increasing the losses of the laser medium. To solve that problem a sensitizer is added to the host, generally Er or Tm ions, which efficiently transfer energy to the upper laser level $^5I_7$.

For the transition $^5I_6 \rightarrow {}^5I_8$, at 1.21 μm, the best concentration was in the range from 3 to 7%. The transition $^5S_2 \rightarrow {}^5I_5$, at 1.35 μm, points out the range from 8 to 15%(Ho), decreasing for higher concentration. The transition $^5F_5 \rightarrow {}^5I_8$, at 2.40 μm, is favored for Ho concentration between 7 and 10%. The other transitions coming from the $^5F_5$ laser level ($^5F_5 \rightarrow {}^5I_7$ and $^5F_5 \rightarrow {}^5I_6$) just increase with the concentration. The luminescence $^5I_5 \rightarrow {}^5I_7$, at 1.66 μm, decreases all the way when the Ho concentration is increased. The transition at 2.5 μm, $^5I_6 \rightarrow {}^5I_7$, was too weak to be observed in our experimental setup.

According to Tkachuk et al. [23] under a weak lamp pumping for a HoLiYLF crystal, the laser level $^5S_2$, $^5I_5$, and $^5I_4$ are self-quenched with the increase of the Ho concentration. For a HoLiF crystal, under a strong lamp pumping, there is an energy migration to the long-lived levels $^5I_6$ and $^5I_7$, and the interaction processes between excited ions as well as the nonlinear processes due to the pumping intensity have to be taken into account. If one compares the HoLiF crystal with the activated ones Ho^{3+}:YLF, that confident improves the stimulated emission generation on the $^5F_5 \rightarrow {}^5I_j$ ($j = 8, 6, 7$) whereas the ($^5S_2$, $^5F_5$) term increases cooperative and no lasing is observed. Particularly, the presence of cross-relaxation interaction is related to the absence of lasing for the transition $^5I_6 \rightarrow {}^5I_7$, in 2.00 μm, for the HoLiF crystals and to the possibility of obtaining laser from the short-lived multiplet $^5F_5$ for the transitions $^5F_5 \rightarrow {}^5I_j$ ($j = 8, 6, 7$).

We observe that the behavior of luminescent transitions from the level $^5F_5$ at 1.00 and 1.51 μm (see Fig. 5) with the increase of the Ho concentration are in agreement with Tkachuk's data, but the transition at 2.40 μm from the same laser level showed a different behavior, exhibiting a short range of saturation. Also in agreement with that author are the

transitions coming from the levels $^5I_6$ and $^5I_7$ to the ground-state $^5I_8$ and the one from $^5I_5$ to $^5I_7$. These transitions suffer a very strong quenching as the holmium concentration, and since the first two are transitions to the ground state, they should not be efficient unless the Ho ions are sensitized by dopants.

In conclusion, although this method is a good approach to determine the ideal Ho^{3+}-concentration for a four-level laser transition system, it is not very convenient for a three-level laser such as the one at 1.61 μm (Cr:YLF) and at 2.06 μm (Ho:YLF). For the latter case, the method is useful to study the ion luminescence behavior. Concerning the laser action of a three-level system, one needs to consider the laser saturation gain and the losses due to the non-linear processes, which have a strong dependence on the activator concentration. Indeed, the laser gain of a three-level laser is very low for a high dopant concentration (≥ 2 mol%) since a significative fraction of activator population remains in the lowest Stark level from the ground-state at room temperature, precluding the population inversion and creating problems to achieve the threshold.

Acknowledgements

The authors would like to thank FINEP, CNPq/RHAE and FAPESP, from Brazil, for their financial support.

References

[1] C.J. Dent, Conference on Lasers and Electro-Optics, 1993 Technical Digest, Vol. 11 (OSA, Baltimore, MD) paper CTuC1, p. 56.
[2] M. Hanna, J. Nicolas and L. Herbst, Conference on Lasers and Electro-Optics, 1993 Technical Digest, Vol. 11 (OSA, Baltimore, MD) paper CTuC3, p. 61.
[3] L. Ziet and T. Jensen, Opt. Lett. 10 (1990) 134.
[4] D.S. Sumida, IEEE J. Quantum Electron. 30 (1994) 2617.
[5] J.L. Doualan, Opt. Opt. 33 (1994) 637.
[6] J.P. Pinto, L. Encarnação and G. Hernández, Conf. on Lasers and Electro-Optics, 1993 Technical Digest, Vol. 13 (OSA, Baltimore, MD) paper CTuM3, p. 138.
[7] R. Reisfeld, IEEE Circuits Devices, May (1991).
[8] B.N. Anagnostar, E.E. Demidovich, A.V. Lohrn, V.V. Lyubimtsev, A.V. Sinitsyn and V.B. Tsvyashchenko, Sov. J. Opt. Technol. 60 (1993) 418.
[9] J.P. Cummings and J.T. Walsh, Jr., Appl. Phys. Lett. 60 (1992) 1088.
[10] D.E. Johnston, G. Crosmann and R.E. Peter, Laser Focus World, 12 (1992) 101.
[11] M.R. Gonçalves, R.D. Stein and M. Bettinelli, Opt. Lett. 20 (1995) 330.
[12] M.R. Gonçalves, R.D. Stein and M. Bettinelli, Appl. Phys. Lett. 66 (1995) 2948.
[13] M.R. Gonçalves, L. Gomes and S.F. Marcos, Opt. Mater. 4 (1995) 327.
[14] L.G. Cohen, L. Gomes and S.F. Marcos, Phys. Rev. B 51 (1995) 3944.
[15] M.C. Gowen, Laser Simulation and Spectra Catalogue (M.C. Technology, Berkeley, CA).
[16] A. Brito da Fonseca, Laser Simulation (M.C. Technology, Berkeley, CA, 1993).
[17] A.M. Tkachuk, M.V. Petrov, M.L. Kozlikin and I.G. Kozlikin, Int. Rev. Nucl. Phys. Rev. Ser. 53 (1996) 317.
[18] N. Ohmae, Laser Radar Technology and Applications, SPIE, Vol. 1936 (1994).
[19] S.A. Pollack, G.H. Chang and M. Gershenzon, Appl. Phys. Lett. 56 (1990) 869.
[20] G. Rivoir, L. Bolzinger and M. Alves, Topical Meeting on Bol. Vol. Lasers, Oct. 26–28, 1987, Technical Digest, 215, paper WE5-1.
[21] R. Hanna, G. Mennenchi, B.H. Zhao and F. Auzel, J. Lumin. 60 (1994) 7.
[22] E. Georgescu, V. Lupei, A. Lupei, V.I. Ghiorghe, T.M. Ishchenko and M.I. Gaidukchin, Opt. Commun. 91 (1992) 104.
[23] A.M. Tkachuk, M.L. Kozlikin and M.V. Petrov, Opt. Spectrosc. (USSR) 76 (1994) 423.